

## Article

# Characteristics and Controlling Factors of Natural Fractures in Continental Tight-Oil Shale Reservoir

Xiaofei Fu <sup>1</sup>, Lei Gong <sup>2,\*</sup>, Xiaocen Su <sup>3</sup>, Bo Liu <sup>1</sup> , Shuai Gao <sup>2,\*</sup>, Jianguo Yang <sup>4</sup> and Xinnan Qin <sup>3</sup>

<sup>1</sup> Key Laboratory of Continental Shale Hydrocarbon Accumulation and Efficient Development, Ministry of Education, Northeast Petroleum University, Daqing 163318, China

<sup>2</sup> Bohai-Rim Energy Research Institute, Northeast Petroleum University, Qinhuangdao 066004, China

<sup>3</sup> College of Geosciences, Northeast Petroleum University, Daqing 163318, China

<sup>4</sup> Shenyang Center of China Geological Survey, Shenyang 110034, China

\* Correspondence: kcgonglei@nepu.edu.cn (L.G.); gaoshuai@nepu.edu.cn (S.G.)

**Abstract:** Natural fracture growth plays an important role in shale-oil enrichment. Systematically investigating fracture features and their controlling factors in shale-oil reservoirs is essential for accurately predicting fracture distribution. The controlling factors of fracture distribution in the continental shale of the Qingshankou Formation in the Songliao Basin, China, were systematically analyzed based on the quantitative fracture characterization of outcrops and cores. Strata-confined fractures, throughgoing fractures, bedding-parallel fractures, and stylolites can be observed in the Qingshankou shale reservoir in the study area. Fracture distribution is not only controlled by internal factors, e.g., mineral composition, mechanical stratigraphy, and lithofacies, but also by external factors, e.g., faults and abnormally high pressure readings. Mineral composition is the primary factor governing fracture development, and it not only controls fracture abundance, but it also affects fracture filling and effectiveness. Mechanical stratigraphy determines the spatial morphology and developmental pattern of a fracture. Fractures are well-developed in brittle strata, with fracture spacing being proportional to bed thickness. Lithofacies can determine fracture development by controlling the variation of mineral composition, rock structure, bed thickness, etc. Stress concentration is commonly high at fault tips, intersections, and overlaps, where fracture density is high and has good connectivity. The existence of abnormally high pressure reduces effective stress, promoting shear fracture development. Tensile overpressure fractures can also be generated under small levels of differential stress.

**Keywords:** continental shale; natural fracture; controlling factor; Songliao Basin



**Citation:** Fu, X.; Gong, L.; Su, X.; Liu, B.; Gao, S.; Yang, J.; Qin, X.

Characteristics and Controlling Factors of Natural Fractures in Continental Tight-Oil Shale Reservoir. *Minerals* **2022**, *12*, 1616. <https://doi.org/10.3390/min12121616>

Academic Editor: Ricardo Ferreira Louro Silva

Received: 26 October 2022

Accepted: 6 December 2022

Published: 15 December 2022

**Publisher's Note:** MDPI stays neutral with regard to jurisdictional claims in published maps and institutional affiliations.



**Copyright:** © 2022 by the authors. Licensee MDPI, Basel, Switzerland. This article is an open access article distributed under the terms and conditions of the Creative Commons Attribution (CC BY) license (<https://creativecommons.org/licenses/by/4.0/>).

## 1. Introduction

Shale oil is a new bright spot in global unconventional oil exploration with potential resource prospects [1–4]. It can be divided into fractured shale oil, brittle interlayered shale oil, and matrix shale oil [2,5]. Fractures of various scales are regarded as primary storage spaces in fractured shale-oil reservoirs [6–9]. Fractures are also the key factor that determine whether shale oil can be enriched. In the absence of fractures, it is difficult to obtain natural productivity from shale [2]. The initial production capacity of a fractured shale-oil reservoir is generally high, but it then declines rapidly due to the limited storage space in the fracture system, where oil in matrix pores is important for replenishing productivity [10,11]. Therefore, a fractured reservoir is beneficial for shale-oil discovery at the early exploration stage, while the presence of matrix pores in a shale reservoir is the key to long-term, stable production [12–15]. These two types of storage spaces contribute significantly to shale-oil exploration and development.

Shale-oil resources have been discovered in the north of the Songliao Basin, mainly distributed in the Cretaceous Qingshankou Formation [16]. Currently, 45 wells have been tested in the Qingshankou Formation, while commercial oil flow has been obtained from

25 of them. Previous studies estimated that the Qingshankou Formation shale-oil resource contained 180–440 million tons with a favorable exploration area of up to  $2 \times 10^4$  km<sup>2</sup>, exhibiting huge exploration potential. Systematic research and exploration have been deployed since the shale reservoirs were discovered in the 1980s; the productive experimental area of well Y12 was established, and horizontal well G1 was drilled to improve productivity. In August 2021, Daqing Oilfield announced the discovery of a major strategic breakthrough in shale-oil exploration in the Songliao Basin, which confirmed the prediction that the geological reserves of the shale oil equal 1.268 billion tons. However, the reservoir's characteristics are special: natural fractures control the distribution of high-quality reservoirs. Gong et al. [17] characterized and discussed the effectiveness of fractures in these shale reservoirs, but the main controlling factors of fracture distribution need to be further analyzed. A significant challenge in understanding fractures in the subsurface is the incomplete sampling that is inherent in using wellbores (cores and image logs). It is common for subsurface core-based studies to supplement direct observations of the subsurface by using outcrops as analogs and guides to the subsurface, as the present study does, but the use of such analogs must be undertaken with caution because, inevitably, outcrops have experienced loading and thermal histories different from those of the rocks still in the subsurface. This potential limitation of the use of outcrops needs to be acknowledged, and the possible limitations of conclusions drawn from the subsurface should be acknowledged [18]. This paper focuses on fracture characterization in outcrops, and combined with core fracture characterization and experimental analysis, defines the fracture characteristics in this shale-oil reservoir and discusses the main controlling factors of fractures in this shale-oil reservoir.

## 2. Geological Setting

The Songliao Basin is located in northeast China (Figure 1) and has an area of about  $26 \times 10^4$  km<sup>2</sup> [19]. It is a large, continental depression basin formed during the Late Cretaceous period where dark shale was widely developed during the Qingshankou period [20]. The Qingshankou Formation was deposited during a large-scale lacustrine transgression under a humid and hot environment. It can be divided, from bottom to top, into the Qing-1, Qing-2, and Qing-3 Members. The Qing-1 Member, the target of study in this paper, is dominated by a set of deep lacustrine organic-rich black shale with a large thickness, a high level of organic carbon content (TOC), and moderate maturity in the center of the lake, which was deposited under a rapid lacustrine transgression [21,22]. It is primarily shale, silty shale, argillaceous siltstone, and limestone. The average thickness of the organic-rich shale in the Qing-1 Member is 70–80 m. The TOC is in the range of 1–5%, with an average value of 2.9%. The vitrinite reflectance (Ro) varies between 0.72% and 1.20%, with an average value of 0.91%. After the deposition of the Qing-1 Member, three tectonic events occurred in the study area, and a series of normal faults was formed at the end of the Qing-3 Member, the Nen-2 Member, and the Nen-3 Member, respectively.

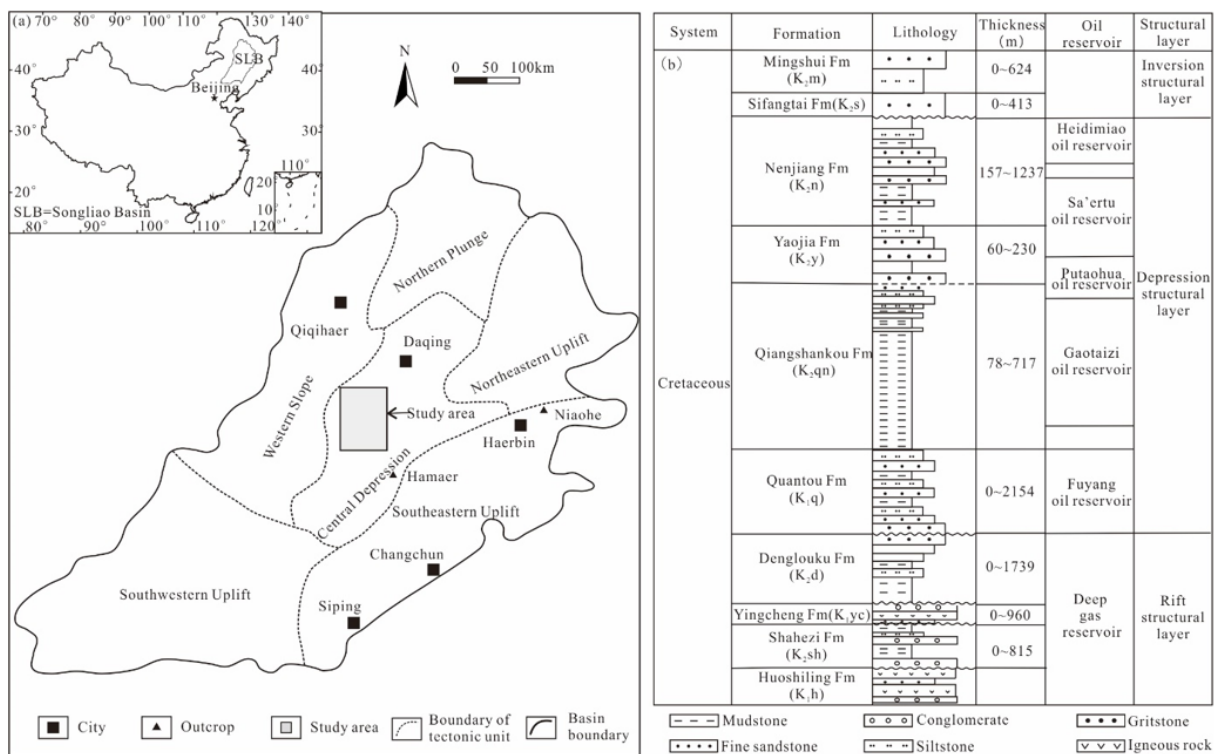


Figure 1. Structural units of the Songliao Basin and the location of the study area.

### 3. Materials and Methods

Outcrop and core fractures were observed and samples were collected to study fracture development and its controlling factors in Qingshankou shale. Two well-exposed outcrops (Niaohe and Hamaer) at the edge of the Songhua River were selected to describe fracture growth in the shale (Figure 1). In addition, 215-meter cores from 5 wells at Songliao Basin were also observed so as to describe fracture growth. The 1D scanline method was used to accurately describe the fractures [23]. Scanlines were arranged in each mechanical layer and were perpendicular to fracture traces. Information (location, occurrence, height, filling property, etc.) about each fracture intersecting with the scanning line was measured and recorded. Fracture intensity was expressed by fracture spacing and fracture density. Specifically, the fracture spacing is the vertical distance between two adjacent fractures, while the fracture density is the number of fractures per meter, which is inversely related to fracture spacing.

Mineral composition analysis, rock mechanical testing, and lithofacies classification were carried out to study the controlling factors of fracture development. The whole-rock mineral composition of 18 outcrop samples were analyzed using the X-ray diffraction method; corresponding brittleness indexes (BI) were calculated using the following model: BI = quartz content + carbonate mineral content. The rock mechanical parameters (elastic modulus, Poisson’s ratio, and compressive strength) of 9 core plugs were tested on a TAW-2000 triaxial rock compression test system at Northeast Petroleum University. The three-step classification criteria proposed by Liu et al. [2] were adopted for the lithofacies classification.

### 4. Fracture Characterization

#### 4.1. Fracture Types and Characteristics

Four types of fractures were identified in the Qingshankou Formation, namely, strata-confined fractures, throughgoing fractures, bedding-parallel fractures and stylolites.

Strata-confined fractures refer to fractures that develop in a single layer and end at a lithologic interface or a bedding surface [24] whose distribution is controlled by mechanical

stratigraphy (Figure 2a). Strata-confined fractures are widely developed, commonly run parallel to each other, and end at the layer interface. They are nearly perpendicular to the bedding surface, and consequently, their heights are generally equal to the bed thickness. These strata-confined fractures appear to be equally spaced on the outcrops. However, data from horizontal wells show that fractures at this depth are highly clustered (not regularly spaced), whereas the same fracture sets in outcrops of the same unit have regular spacing [25]. The reason for the difference is that fractures forming in the deep subsurface are subject to different chemical effects [18,26].

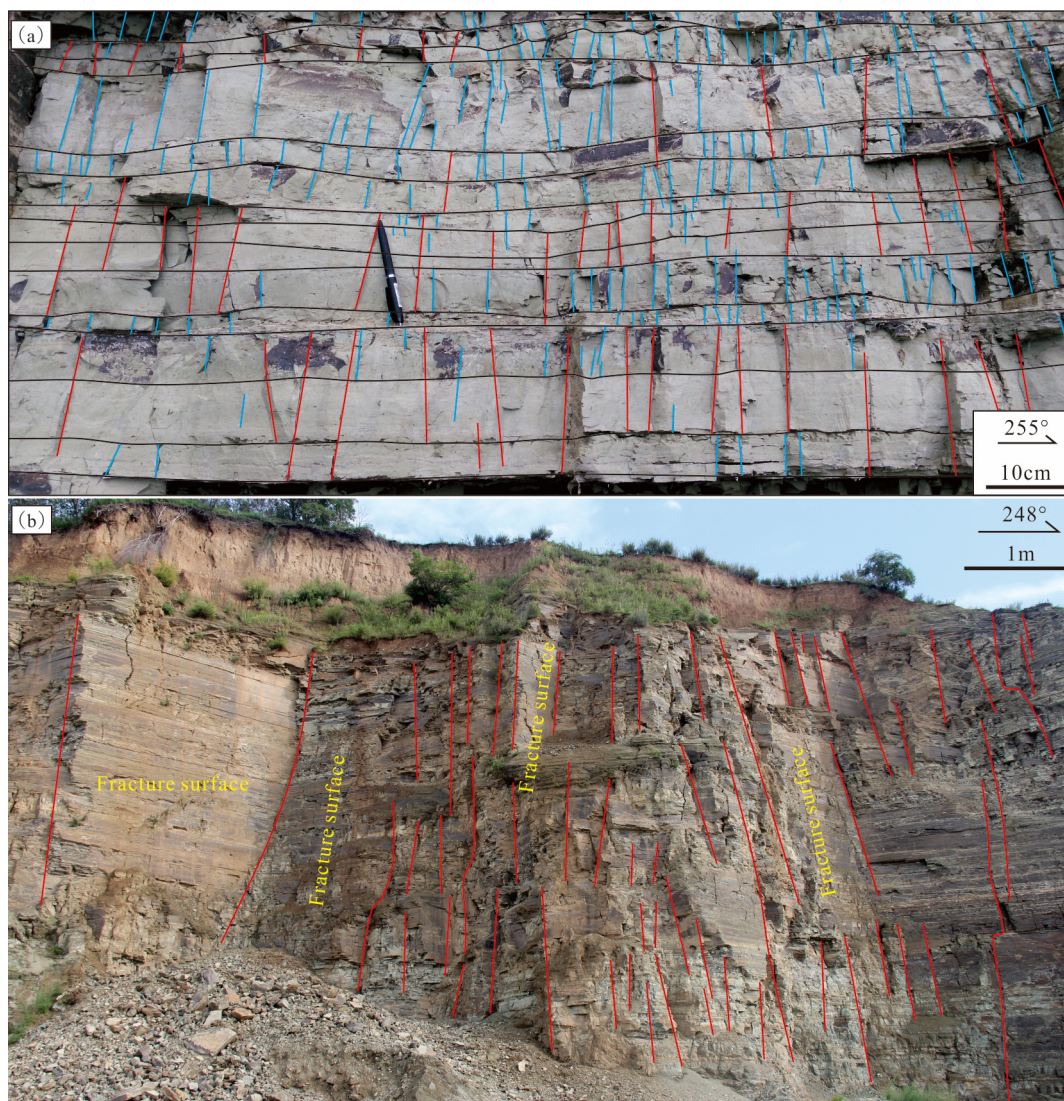


**Figure 2.** (a) Strata-confined fractures (blue lines) and throughgoing fractures (red lines); (b) throughgoing fractures (red lines).

Throughgoing fractures can develop in different patterns, e.g., as a single fracture or as high-density and nearly parallel-oriented fracture groups [27–30]. They tend to extend across multiple mechanical units, occurring as multilayered structures (Figure 2b). The throughgoing fractures have a steep dip or are even vertical, while their strikes are consistent with those of the strata-confined fractures. Many fracture segments in throughgoing fracture are single strata-confined, and they are widened or interconnected at the bedding surface to form throughgoing fractures. These throughgoing fractures are also equally spaced, indicating that they are universally penetrative structures rather than isolated or

local structures [31,32]. Furthermore, they are commonly formed within the same tectonic stress field.

The bedding-parallel fractures in shale were formed by slow deposition under relatively stable hydrodynamic conditions, which consist of a series of flat and fine bedding-parallel layers. Bedding-parallel fractures are usually non-structural fractures caused by diagenesis, e.g., compaction, cementation, and clay mineral transformation, that commonly occur along the bedding surface (Figure 3a). Shale bedding is interfaced with a weak mechanical property and easily peels off to become a bedding-parallel fracture. These bedding-parallel fractures are well-developed in organic-rich shales and are commonly perpendicular to the overburden pressure, occurring as closed fractures.

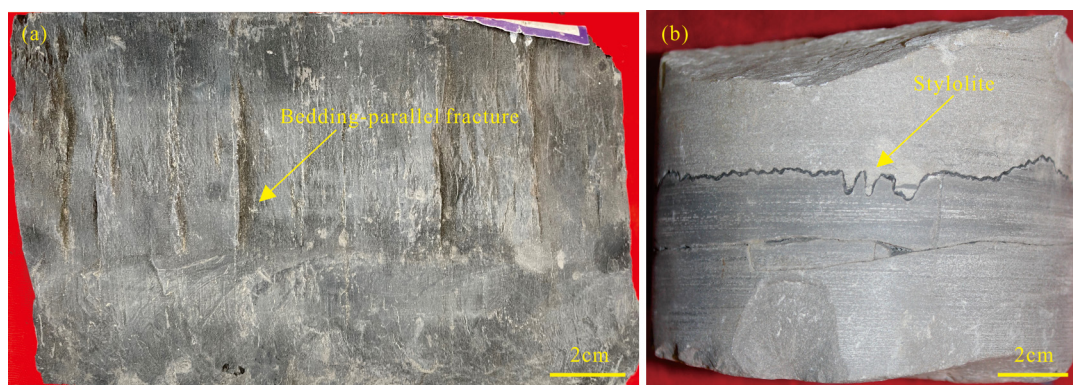


**Figure 3.** (a) Bedding-parallel fractures; (b) stylolite.

The stylolites occur as serrated or columnar fractures filled by dark minerals. These serrations or columns are nearly vertical and are perpendicular to the fracture surface (Figure 3b), suggesting that they are diagenetic stylolites. They have an uneven surface that is parallel to the bedding surface, indicating that they are formed by a pressurized solution, where insoluble minerals are retained and soluble minerals are taken away by fluid. Most stylolites are typical seepage barriers since they are filled by insoluble material.

#### 4.2. Quantitative Fracture Characterization

Field measurements show three sets of fractures in the study area, e.g., NNW–SSE trending, NE–SW trending, and NEE–SWW trending (Figure 4a). Fractures with a high dip angle are the most important, e.g., fractures with a dip angle  $> 70^\circ$  account for more than 93% of the total (Figure 4b). Fractures in the core are also high-dip, while a few oblique fractures and low-dip fractures are also developed.

Fractures in the Qingshankou Formation are well-developed, especially in the fault zone. Fracture spacing in outcrops is mainly 5–20 cm, while fracture density is  $5\text{--}12.5\text{ m}^{-1}$ . Fracture density in the core is about  $0.3\text{--}1.0\text{ m}^{-1}$ , with a maximum value of  $1.52\text{ m}^{-1}$ . The ratio of total fracture height to core length is generally less than 0.1, with an average value of 0.05.

The height of the strata-confined fractures in the outcrops ranges from 10 to 40 cm, following a normal distribution pattern. The height of throughgoing fractures is the range of 50–200 cm, which is also normally distributed. However, the height of all of the fractures (strata-confined fractures and throughgoing fractures) obeys a power law distribution, indicating that they are formed under a uniform tectonic stress field. The fracture height in the core is generally less than 20 cm due to mechanical stratigraphy, while the maximum value of a few of the fractures, which penetrate multiple layers, can be up to 2.8 m.

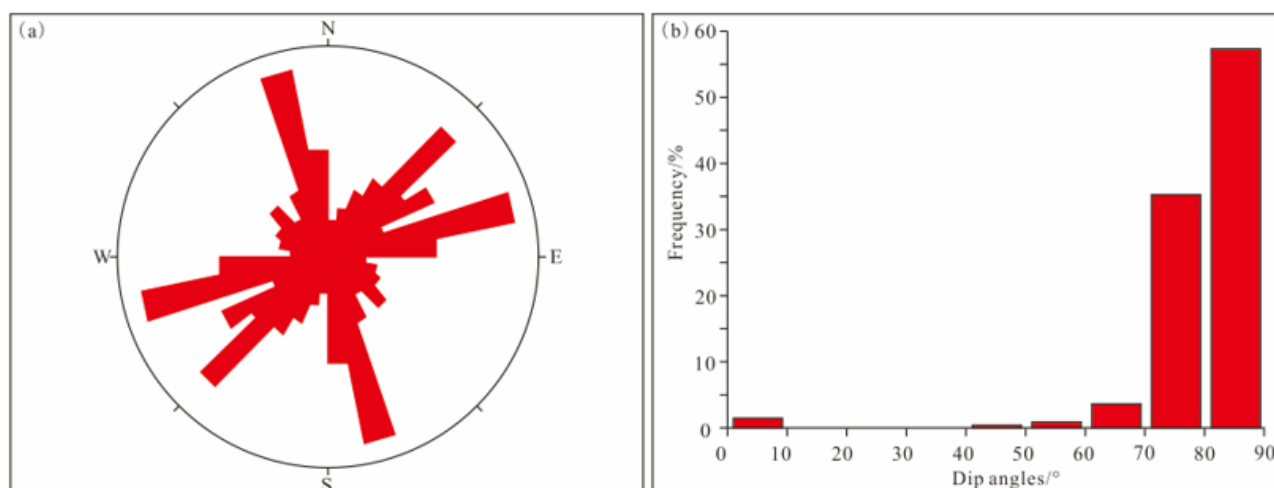


**Figure 4.** (a) Rose diagram of fracture strikes; (b) histogram of dip angles in outcrops.

Most fractures are filled by different minerals (calcite, quartz, and bitumen); specifically, fully-filled, half-filled and unfilled fractures account for 59%, 16%, and 25%, respectively. The half-filled and unfilled fractures are effective ones, while the fully-filled fractures have weak surfaces that are conducive to hydrofracturing.

## 5. Discussion

Fracture development varies greatly in different positions in the shale due to strong heterogeneity. The unevenly developed fractures bring great challenges to the study of tight shale reservoirs and significantly increase oil/gas exploration and development risks in such reservoirs. Although fracturing is complex and heterogeneous in distribution, its occurrence commonly follows certain rules. Geological factors controlling fracture formation and distribution are discussed based on outcrop, core, and thin section observation and experimental analysis, which provides an insight into fracture prediction in shale.

### 5.1. Mineral Composition and Content

Lithology is the most basic factor influencing fracture development in tight reservoirs [33,34] since mineral composition, texture, and structure, as well as mechanical properties, vary greatly with lithology [35,36]. Therefore, fracture development is different in various forms of lithology under the same tectonic stress [37]. The influence of mineral composition, rock mechanical properties, and brittleness on fracture development was analyzed based on X-ray diffraction analysis and rock mechanical tests.

Fracture line density is positively correlated with quartz content and carbonate mineral content (Figure 5a,b), but it is negatively correlated with clay mineral content (Figure 5c). However, an obscure relationship occurs between feldspar content and fracture development (Figure 4d). These phenomena indicate that, under the same tectonic stress, fractures can be well-developed in brittle rocks with a high content of quartz, calcite, and dolomites, but it can be poorly developed in ductile rocks with high levels of clay minerals (Figure 6). Additionally, fractures in shale with high carbonate mineral content are usually fully filled with calcite [1,38,39], while fractures in shale dominated by quartz and feldspar are weakly filled, commonly unfilled, or half-filled by euhedral quartz (Figures 6 and 7).

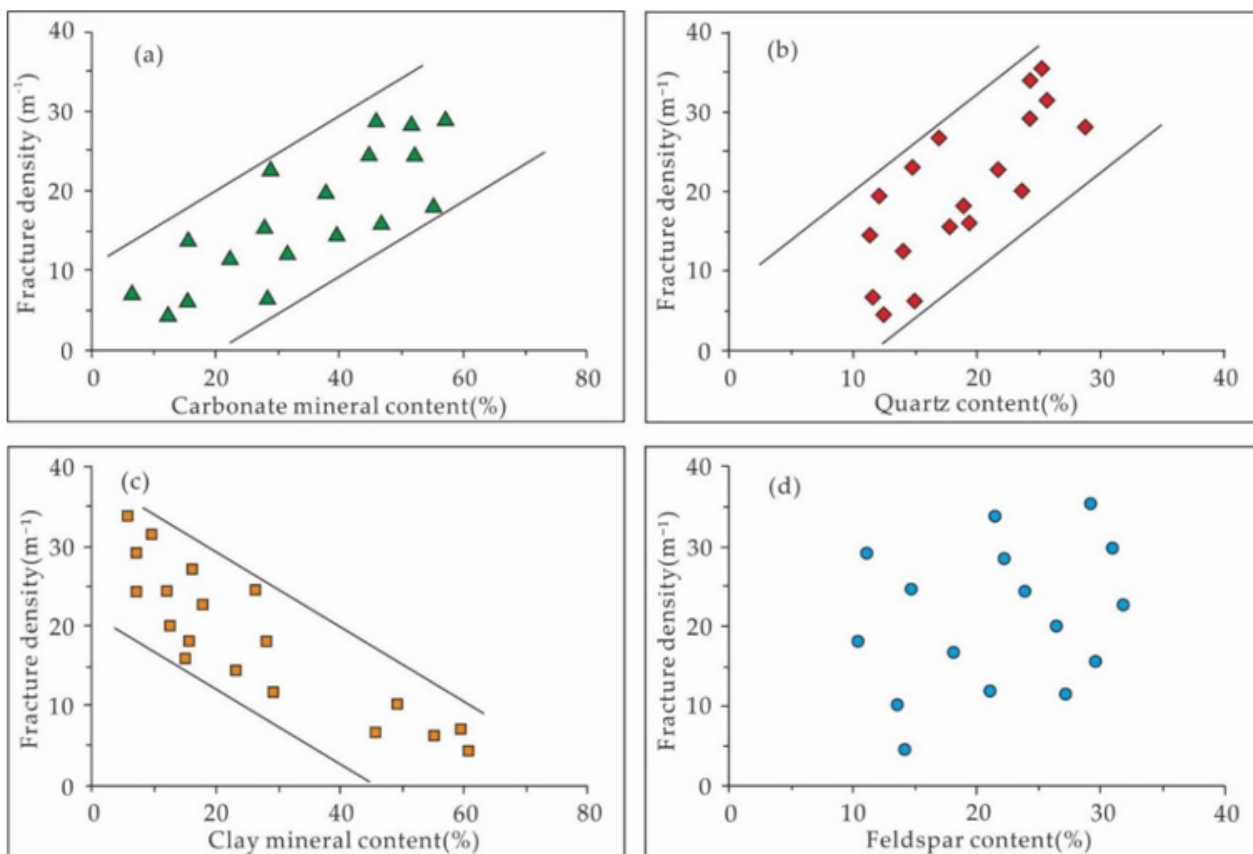


**Figure 5.** Relationship between different mineral contents and fracture density in Qingshankou shale. (a) Carbonate mineral content vs. fracture density; (b) quartz content vs. fracture density; (c) clay mineral content vs. fracture density; (d) feldspar content vs. fracture density. Samples were collected from outcrops.

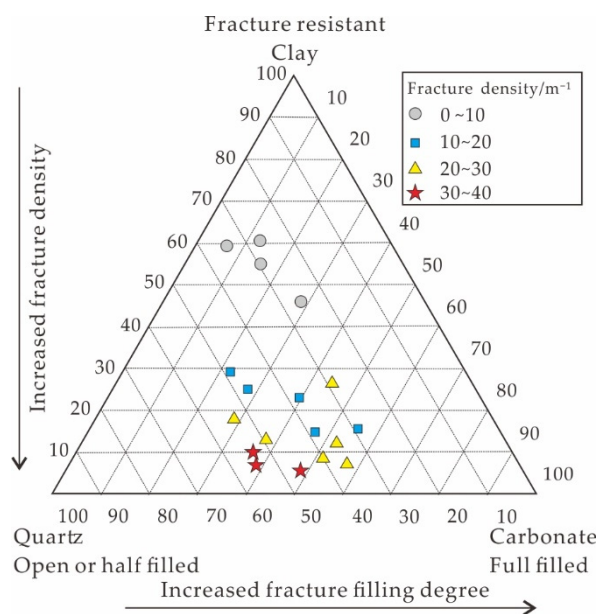


**Figure 6.** Host rock mineral composition and fracture distribution. Samples were collected from outcrops.

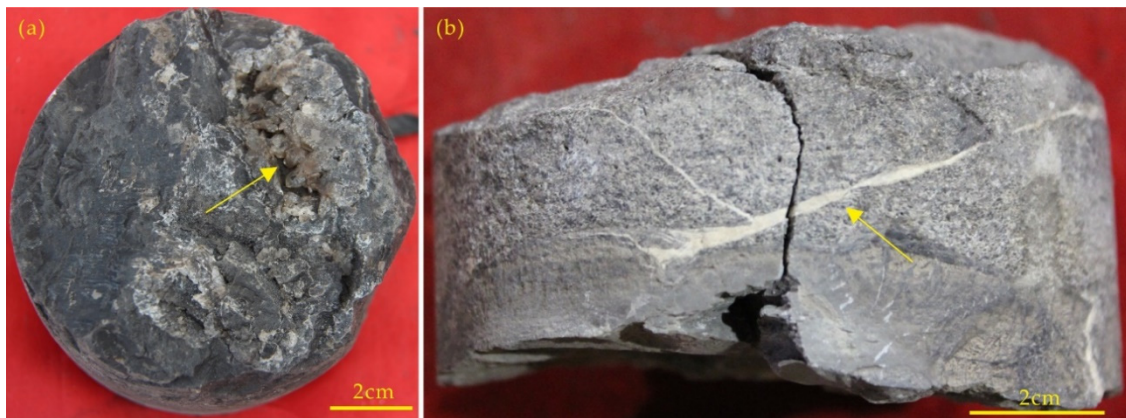


**Figure 7.** Images showing fractures with different fillings: (a) fracture half-filled with euhedral quartz; (b) fracture fully filled with calcite. The yellow arrows indicate the location of the fractures.

The brittleness index (BI = quartz content + carbonate mineral content) was calculated to analyze its relationship with fracture density. The results show that fracture development has a better correlation with the BI compared with single-mineral content (Figure 8), suggesting that the brittleness index is a good indicator of fracture growth. Consequently, the rock brittleness index can be used as a constraint when predicting fracture development.

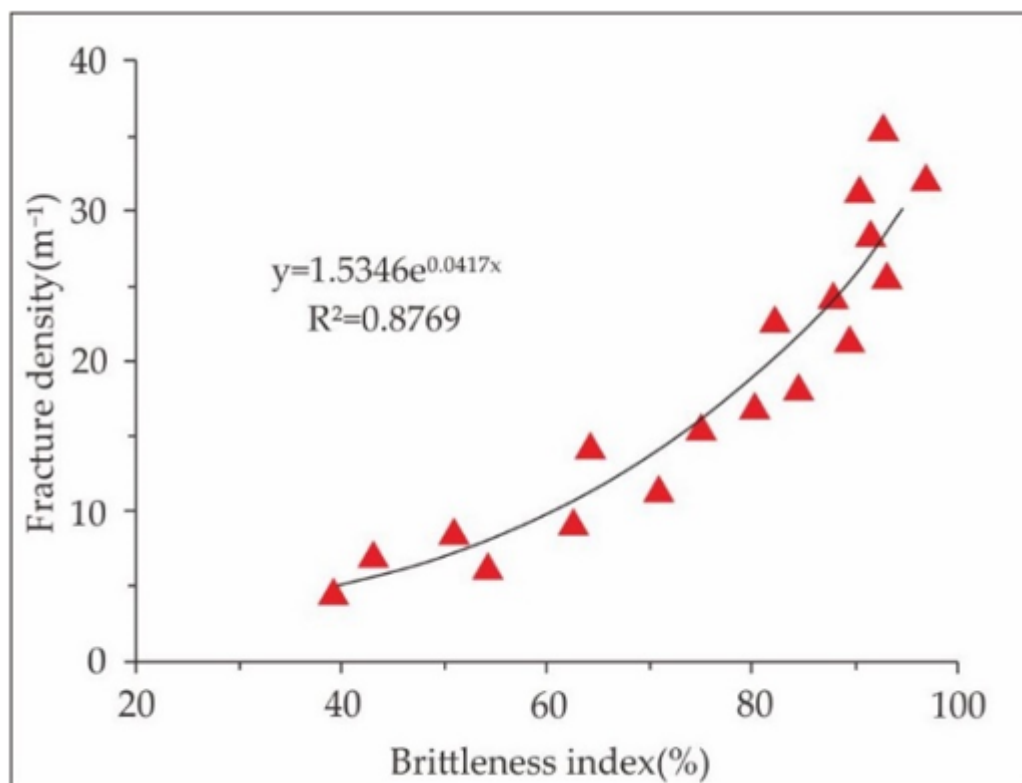


**Figure 8.** Relationship between brittleness index and fracture density in Qingshankou shale. Samples were collected from outcrops.

Under the same stress field, the fracture development is mainly governed by rock mechanical properties (such as the elasticity modulus, Poisson's ratio, the bulk modulus, compressive strength, etc.). Fracture intensity in different lithologies vary greatly within these parameters. Comparing fracture development and rock mechanical parameters shows that the fracture development is in a mirror-image relationship (inverse ratio) with the

compressive strength and Poisson's ratio, and it is positively correlated with the elasticity modulus and the bulk modulus. In other words, lower levels of compressive strength and Poisson's ratio and a larger elasticity modulus are beneficial for fracture development (Figure 9).

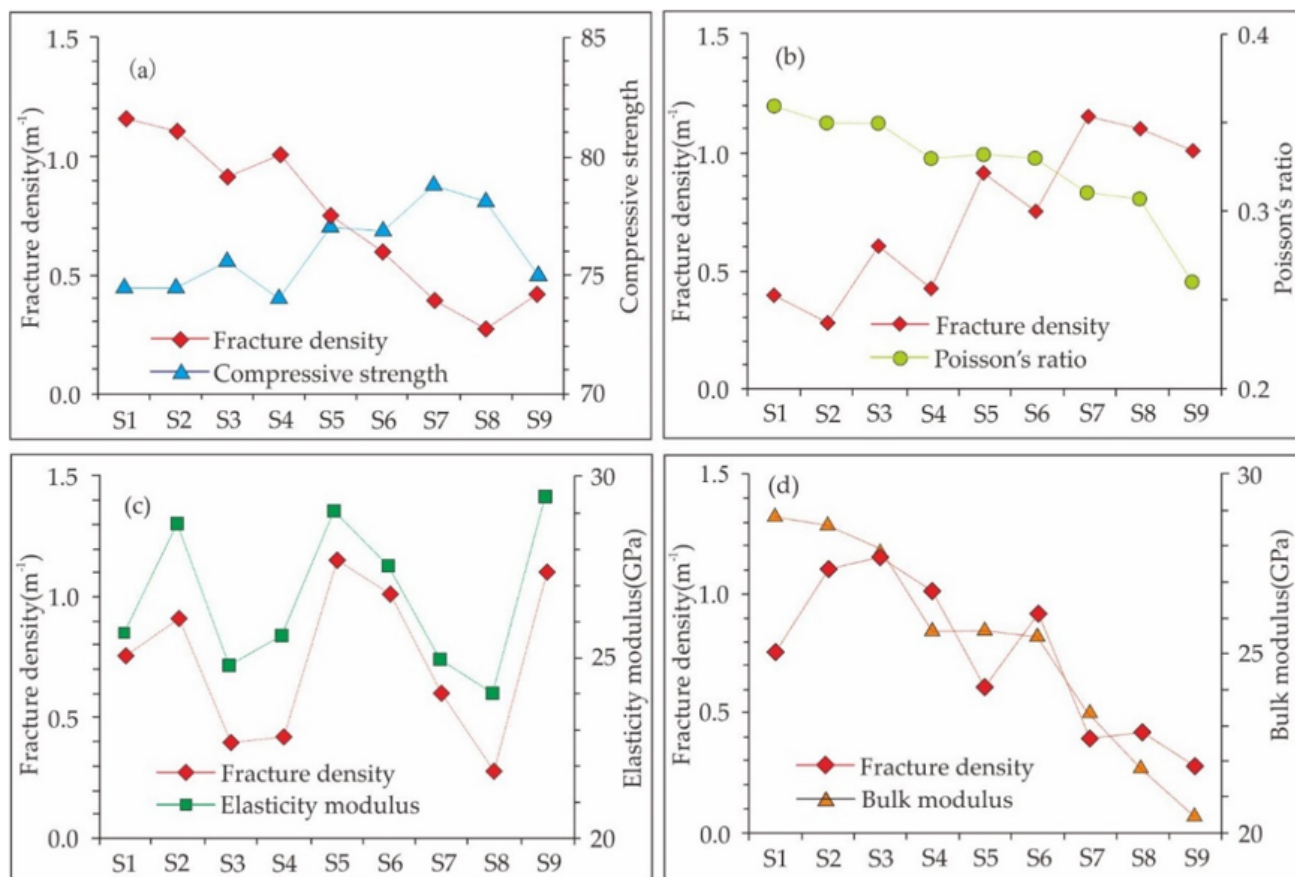


**Figure 9.** Relationship between rock mechanical parameters and fracture density in Qingshankou shale: (a) Compressive strength vs. fracture density; (b) elasticity modulus vs. fracture density; (c) Poisson's ratio vs. fracture density; (d) Bulk modulus vs. fracture density. Samples were collected from cores. The 9 samples have been marked as S1–S9, respectively.

### 5.2. Mechanical Stratigraphy

Fracture observations on outcrops and cores prove that mechanical stratigraphy is one of the most important factors controlling natural fracture types, nucleation, propagation, geometry, and spatial distribution [7,11,40–42]. Previous studies point out that mechanical stratigraphy controls the formation and distribution of natural fractures [43,44].

On the one hand, mechanical stratigraphy controls fracture morphology and developmental pattern [45,46]. Fractures are usually nucleated at defects (e.g., fossil inclusions, pyrite concretions, pores, and cusps) along mechanical interfaces, then spread into the brittle strata, and eventually terminate at the interface between brittle and ductile strata [47,48]. In a relatively homogeneous lamelleted rock, fractures may also end at the mechanical interface and deflect due to interbedded sliding and/or debonding along the interface [49]. These fractures that are limited by mechanical layers are called strata-confined fractures. In the same mechanical layer, strata-confined fractures have equal spacing that follows a normal distribution. On the other hand, mechanical layer thickness controls fracture abundance [48,50]. The statistics on two observation outcrops in Songliao Basin show that the fracture spacing has a good linear relationship with the mechanical layer thickness; that is, the average fracture spacing is proportional to the mechanical layer thickness (Figure 10). Therefore, it is of great significance to establish a relationship between fracture density and

mechanical layer thickness to understand fracture geometry and spatial distribution in different strata units, which is helpful for fracture prediction at subsurface [45,51,52].

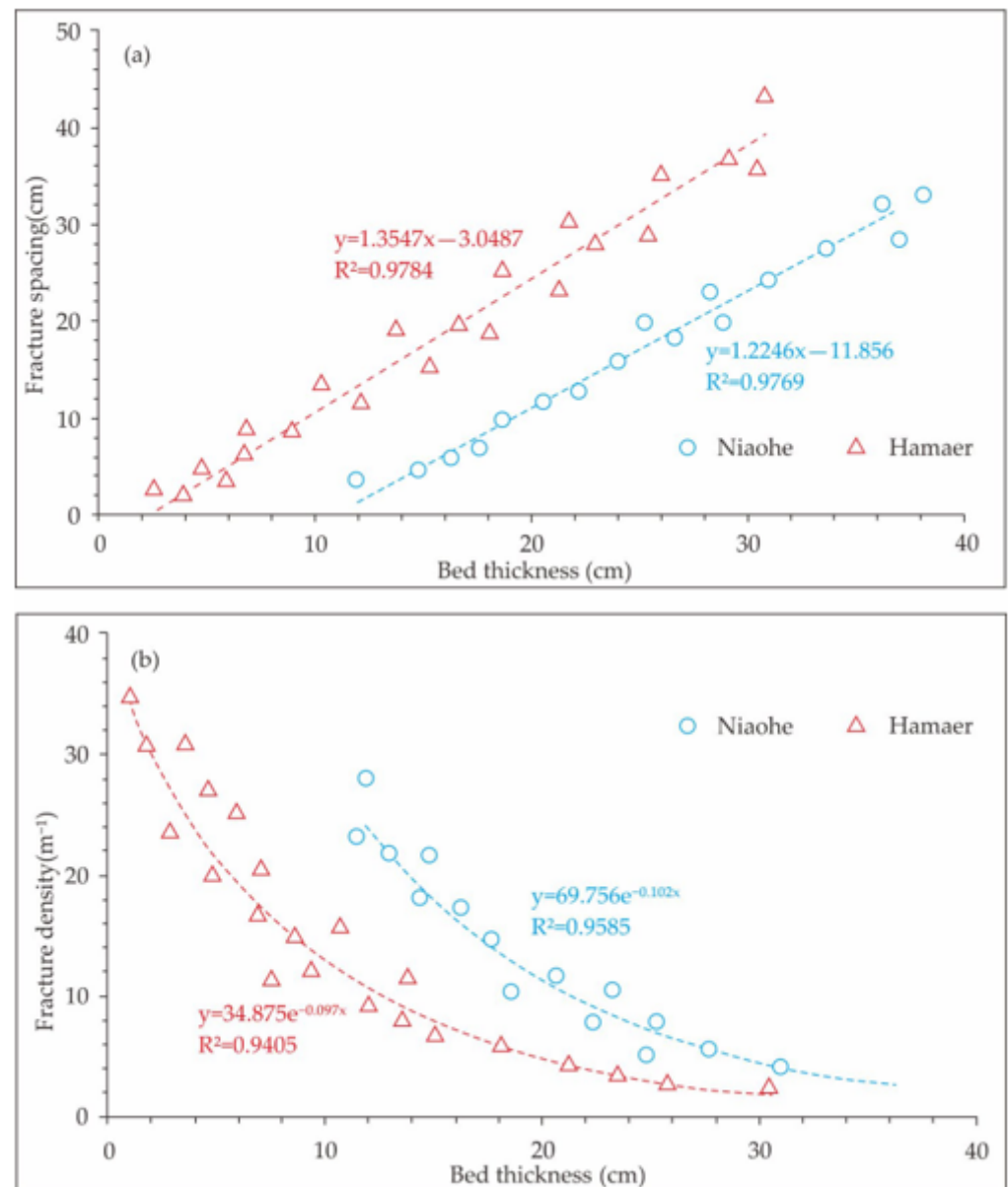


**Figure 10.** Impacts of mechanical layer thickness on fracture intensity in Qingshankou shale: (a) Mechanical layer thickness vs. fracture spacing; (b) Mechanical layer thickness vs. fracture density. NHT-1, NHT-2, NHT-3, and YHT-1 represent survey locations, respectively.

Meanwhile, mechanical stratigraphy also controls fault nucleation, the fracturing mode, fault geometry, the displacement gradient and distribution, segment growth, the fault core and damage zone, and the deformation process [48,52]. The mechanical properties of the host rock and mechanical stratigraphy division are important for fault interpretation, internal structure, and seal property characterization [53,54].

### 5.3. Lithofacies

Lithofacies determines fracture development by controlling TOC, mineral composition, rock structure, and mechanical layer thickness [2]. Seven types of lithofacies were identified in the Qingshankou Formation based on the three-step classification criteria of “total organic carbon abundance—sedimentary structure—mineral composition” [2], i.e.,

type I: high TOC massive siliceous shale; type II: medium TOC massive siliceous shale; type III: medium TOC laminated siliceous shale; type IV: low TOC laminated siliceous shale; type V: low TOC lamelleted siltstone; type VI: low TOC lamelleted limestone; and type VII: high TOC massive argillaceous shale.

Statistical analysis of the fracture development in different lithofacies shows that fractures are well-developed in medium TOC laminated siliceous shale (type III), low TOC lamelleted siltstone (type V), and low TOC lamelleted limestone (type VI), with an average fracture density  $> 1.0 \text{ m}^{-1}$  (Figure 11). Fractures are moderately developed in low TOC laminated siliceous shale (type IV), with an average fracture density of  $0.93 \text{ m}^{-1}$ . They are poorly developed in high TOC massive siliceous shale (type I), medium TOC massive siliceous shale (type II), and high TOC massive argillaceous shale (type VII), especially in high TOC massive argillaceous shale (type VII), where the average fracture density is only  $0.35 \text{ m}^{-1}$ . This indicates that mineral composition is the most important factor controlling fracture development, e.g., quartz and carbonate mineral contents determine fracture development by controlling rock brittleness. Single mechanical layers in laminar shale are lower in thickness, where the fracture density is obviously higher in comparison with massive shale. Under the same conditions, a high TOC can result in a higher fracture density in shale.

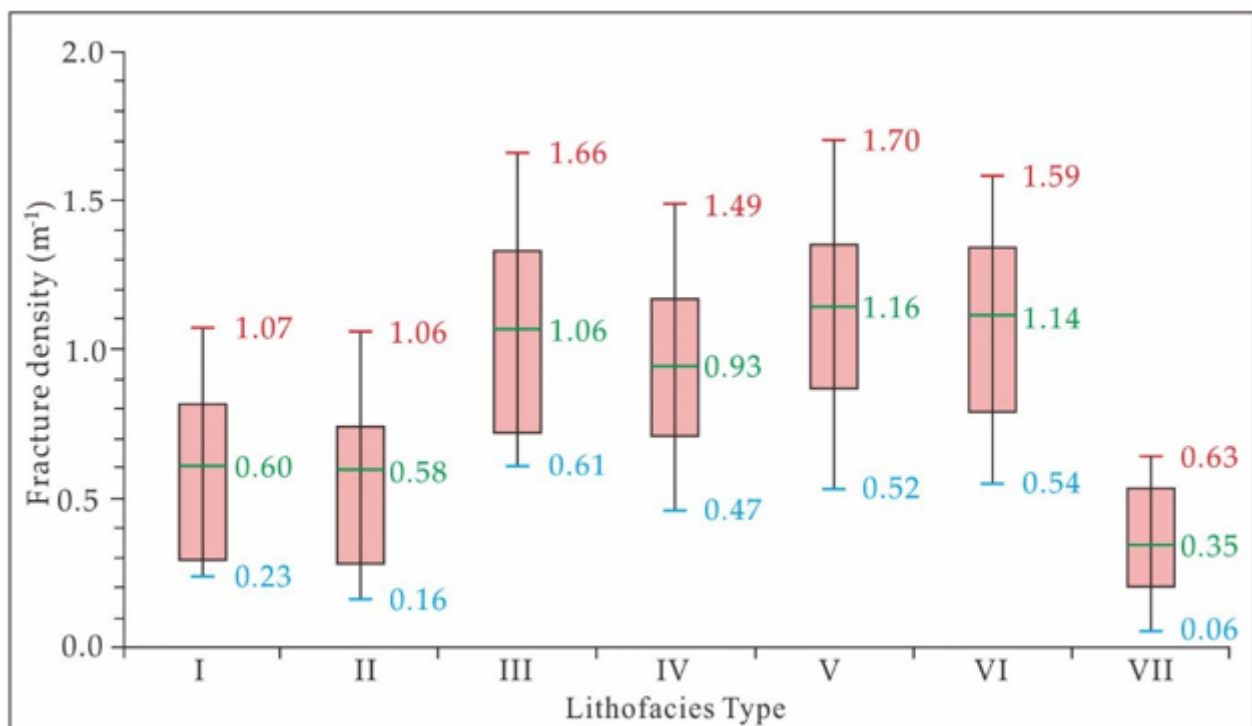


**Figure 11.** Fracture density in different lithofacies: Type I: high TOC massive siliceous shale; type II: medium TOC massive siliceous shale; type III: medium TOC laminated siliceous shale; type IV: low TOC laminated siliceous shale; type V: low TOC lamelleted siltstone; type VI: low TOC lamelleted limestone; and type VII: high TOC massive argillaceous shale. The short red, green, and blue lines represent the maximum, average, and minimum fracture densities, respectively.

#### 5.4. Fault

It is generally recognized that a fault zone has a dual structure, including a fault core and a surrounding damage zone [55,56]. The fault core is generally composed of the sliding surface, fault gouge, breccia, and tectonic lens, while the damage zone is generally composed of fractures of different scales and secondary faults [57–59]. Fault-controlling stress distribution in different positions is an important external factor for determining

fracture development in the Qingshankou Formation. For example, an obvious stress concentration along a fault zone increases the fracture density significantly.

Four small faults can be found at two outcrops. Figure 12a shows two small, normal faults at the Niaohetun outcrop, forming a small graben structure. The first fault (F1) is 20 cm in throw with azimuth and dip angle of  $235^\circ$  and  $42^\circ$ , respectively. The second fault (F2) is 10 cm in throw with azimuth and dip angle of  $52^\circ$  and  $42^\circ$ , respectively. These faults can be divided into fault cores and damage zones, while the fault core is composed of fault breccia (Figure 12b) and structural lens (Figure 12c) with a thickness of 5–10 cm, which is a highly permeable seepage channel. A large number of fractures have developed in the damage zone. Fracture density decreases with the increase in distance from the fault core.

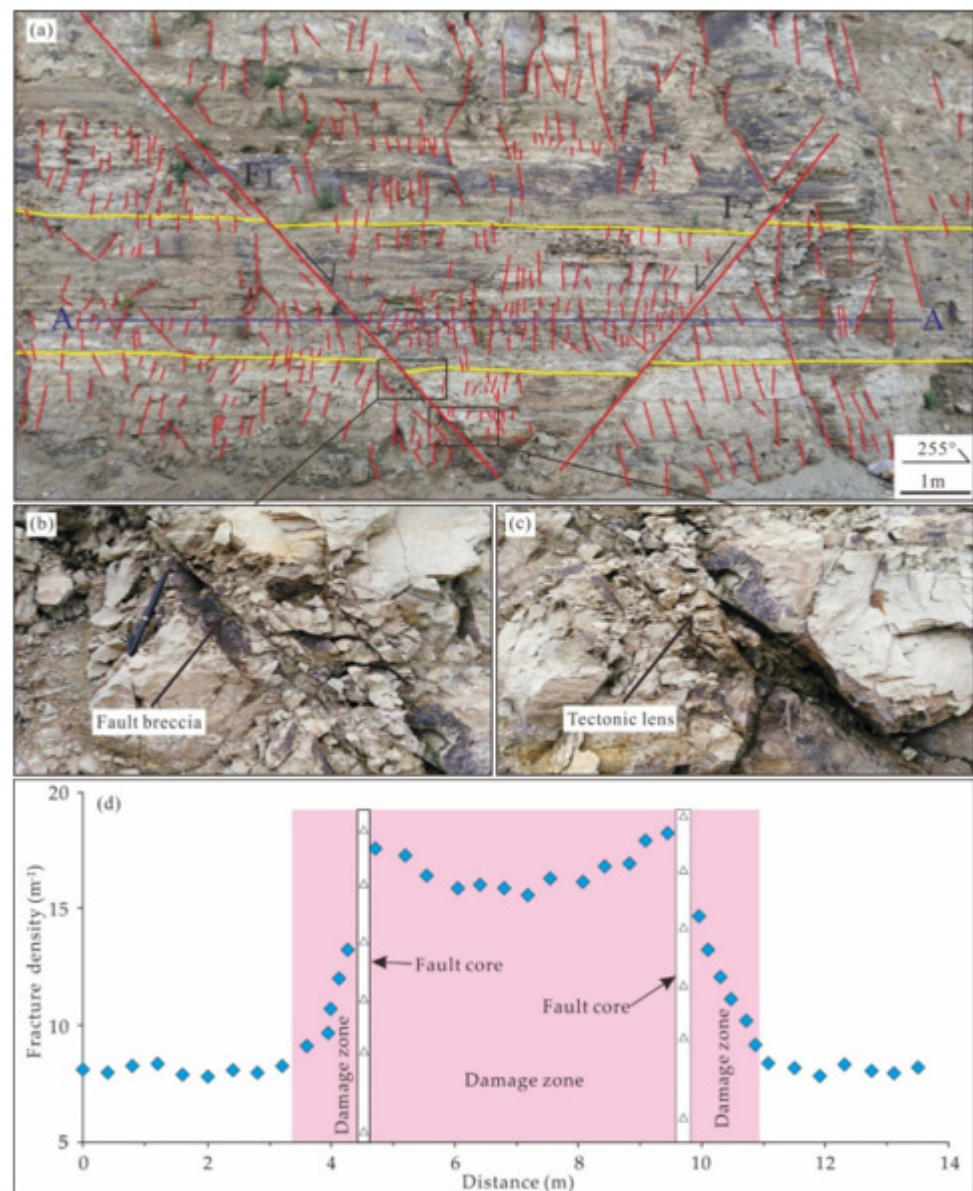


**Figure 12.** Two small, normal faults at Niaohetun outcrop in Bin County, Haerbin City: (a) Photos of these two small, normal faults; (b) fault breccia; (c) tectonic lens; (d) internal structure of fault zone and fracture distribution.

Fracture spacing and density around faults on an outcrop show that fractures have high density and little spacing around fault cores, especially at fault tips, intersections, and overlaps. Fracture density follows an exponentially decreasing trend with an increase in the

distance from the fault core, which tends to be stable at a certain distance (Figure 12d). The boundary of the damage zone can be identified at the position where the fracture density is equal to the regional fracture density. The width of the damage zone is proportional to the fault displacement. However, the growth rate of the damage zone's width decreases when the displacement is higher than a certain value (after a few hundred meters) [60,61]. In addition, a difference in fracture density can be found between two walls; specifically, the fracture density of the hanging wall is significantly higher than that of the foot wall [62]. This can be explained by the fact that the hanging wall is commonly the active one, where stress disturbance is more obvious.

### 5.5. Abnormal High Pressure

Drilling and log data indicate significant abnormally high pressure levels in the Qingshankou Formation, which are caused by under-compaction, hydrocarbon generation, and clay mineral transformation dehydration [2,63]. Abnormally high pressure is an important driving force for fracture development and has an important influence on fracture distribution in shale [64–66].

The existence of abnormal fluid pressure in a reservoir decreases the effective stress when the differential stress is large, moving the stress Mohr circle to the left to intersect with the failure envelope, facilitating the formation of shear fractures (Figure 13, big Mohr circle). Statistical analysis shows a good positive correlation between the fracture density and the formation pressure coefficient, which indicates that the presence of abnormally high pressure contributes to fracture development. This can be explained by the fact that the minimum effective principal stress can vary from compression stress to tensile stress with an increasing pore fluid pressure under small differential stress (Figure 13, small Mohr circle), thus developing tensile fracture.

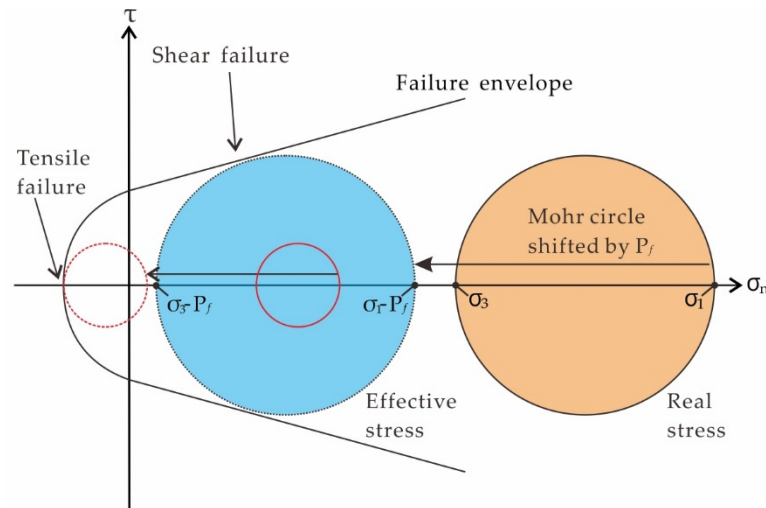


**Figure 13.** Schematic diagram showing formation mechanism for overpressure fractures (modified from Bons et al. [63] and Gong et al. [64]).

## 6. Conclusions

Strata-confined fractures, throughgoing fractures, bedding-parallel fractures, and stylolites were identified in Qingshankou shale. Mineral composition, abnormally high pressure, tectonic position, and mechanical stratigraphy are primarily factors controlling fracture development in shale. High levels of quartz and carbonate mineral content can result in high levels of brittleness, which are beneficial for natural fracture development, while clay minerals are unfavorable to natural fracture development. Fracture development is negatively proportional to compressive strength and Poisson's ratio, and it is positively proportional to Young's modulus and the volume modulus. The existence of abnormally high pressure moves the stress Mohr circle to the left with minimal principal stress be-

coming a negative value, resulting in tensile fractures. Mechanical stratigraphy is another factor controlling fracture formation and distribution, e.g., fracture spacing will increase and fracture density will decrease with increases in the mechanical layer thickness. Also, fracture density will decrease with increases in the distance from fault cores. The boundary of the damage zone can be identified at the position where the fracture density is equal to the regional fracture density, which is generally affected by fault size and activity intensity.

**Author Contributions:** X.F.: conceptualization and investigation; L.G.: conceptualization and writing—review and editing; X.S.: data curation; B.L.: formal analysis; S.G.: methodology and original draft preparation; J.Y.: investigation; X.Q.: writing—review and editing. All authors have read and agreed to the published version of the manuscript.

**Funding:** This research was funded by the National Natural Science Foundation of China (grant nos. U20A2093, 42072155, and 41902150); the Natural Science Foundation of Heilongjiang Province (grant no. YQ2022D006); the Young Innovative Talents Training Program for Universities in Heilongjiang Province (grant no. UNPYSCT-2020147); and the Postdoctoral Scientific Research Developmental Fund of Heilongjiang Province (grant no. LBH-Q21001). The APC was funded by the National Natural Science Foundation of China (grant no. 42072155).

**Data Availability Statement:** The data involved in this paper are all included in the text of the manuscript.

**Acknowledgments:** The authors thank Jianguo Huang and Jiaqi Yao at Northeast Petroleum University for their constructive help.

**Conflicts of Interest:** The authors declare that they have no conflict of interest.

## References

- Gale, J.F.W.; Olson, J.E.; Laubach, S.E. Natural fractures in shale: A review and new observations. *AAPG Bull.* **2014**, *98*, 2165–2216. [[CrossRef](#)]
- Liu, B.; Shi, J.X.; Fu, X.F.; Lyu, Y.F.; Sun, X.D.; Gong, L.; Bai, Y.F. Petrological characteristics and shale oil enrichment of lacustrine fine-grained sedimentary system: A case study of organic-rich shale in first member of Cretaceous Qingshankou Formation in Gulong Sag, Songliao Basin, NE China. *Pet. Explor. Dev.* **2018**, *45*, 884–894. [[CrossRef](#)]
- Luo, Q.Y.; Gong, L.; Qu, Y.S.; Zhang, K.H.; Zhang, G.L.; Wang, S.Z. The tight oil potential of the Lucaogou Formation from the southern Junggar Basin, China. *Fuel* **2018**, *234*, 858–871. [[CrossRef](#)]
- Gao, S.; Zeng, L.B.; Ma, S.Z.; He, Y.H.; Gong, L.; Zhao, X.Y.; Xu, W.G.; Tang, X.M. Quantitative prediction of fractures with different directions in tight sandstone reservoirs. *J. Nat. Gas Geosci.* **2015**, *26*, 427–434.
- Luo, Q.R.; Goodarzi, F.; Zhong, N.N.; Wang, Y.; Qiu, N.S.; Skovsted, C.; Such, V.; Schovsbo, N.H.; Morga, R.; Xu, Y.H.; et al. Graptolites as fossil geo-thermometers and source material of hydrocarbons: An overview of four decades of progress. *Earth-Sci. Rev.* **2020**, *200*, 103000. [[CrossRef](#)]
- Li, Y.G.; Gong, L.; Zeng, L.B.; Ma, L.H.; Yang, H.; Zang, B.J.; Zhu, K.W. Characteristics of fractures and their contribution to the deliverability of tight conglomerate reservoirs in the Jiulongshan Structure, Sichuan Basin. *J. Nat. Gas Ind.* **2012**, *32*, 22–26.
- Gottardi, R.; Mason, S.L. Characterization of the natural fracture system of the Eagle Ford Formation (Val Verde County, Texas). *AAPG Bull.* **2018**, *102*, 1963–1984. [[CrossRef](#)]
- Ladevèze, P.; Séjourné, S.; Rivard, C.; Lavoie, D.; Lefebvre, R.; Rouleau, A. Defining the natural fracture network in a shale gas play and its cover succession: The case of the Utica Shale in eastern Canada. *J. Struct. Geol.* **2018**, *108*, 157–170. [[CrossRef](#)]
- Shovkun, I.; Espinoza, D.N. Geomechanical implications of dissolution of mineralized natural fractures in shale formations. *J. Pet. Sci. Eng.* **2018**, *160*, 555–564. [[CrossRef](#)]
- Zeng, L.B.; Lyu, W.Y.; Li, J.; Zhu, L.F.; Weng, J.Q.; Yue, F.; Zu, K.W. Natural fractures and their influence on shale gas enrichment in Sichuan Basin, China. *J. Nat. Gas Sci. Eng.* **2016**, *30*, 1–9. [[CrossRef](#)]
- Smart, K.J.; Ofoegbu, G.I.; Morris, A.P.; McGinnis, R.N.; Ferrill, D.A. Geomechanical modeling of hydraulic fracturing: Why mechanical stratigraphy, stress state, and pre-existing structure matter. *AAPG Bull.* **2014**, *98*, 2237–2261. [[CrossRef](#)]
- Gale, J.F.W.; Gale, R.M.R.; Holder, J. Natural fractures in the Barnett Shale and their importance for hydraulic fracture treatments. *AAPG Bull.* **2007**, *91*, 603–622. [[CrossRef](#)]
- Luo, Q.; Zhong, N.; Dai, N.; Zhang, W. Graptolite-derived organic matter in the Wufeng–Longmaxi Formations (Upper Ordovician–Lower Silurian) of southeastern Chongqing, China: Implications for gas shale evaluation. *Int. J. Coal Geol.* **2016**, *153*, 87–98. [[CrossRef](#)]
- Yin, S.L.; Feng, K.Y.; Nie, X.; Chen, Q.; Liu, Y.; Wang, P.L. Characterization of marine shale in Western Hubei Province based on unmanned aerial vehicle oblique photographic data. *Adv. Geo-Energy Res.* **2022**, *6*, 252–263. [[CrossRef](#)]

15. Li, B.K.; Nie, X.; Cai, J.C.; Zhou, X.Q.; Whang, C.C.; Han, D.L. U-Net model for multi-component digital rock modeling of shales based on CT and QEMSCAN images. *J. Pet. Sci. Eng.* **2022**, *216*, 110734. [[CrossRef](#)]
16. Liu, B.; Sun, J.H.; Zhang, Y.Q.; He, J.L.; Fu, X.F.; Yang, L.; Xing, J.J.; Zhao, X.Q. Reservoir space and enrichment model of shale oil in the first member of Cretaceous Qingshankou Formation in the Changling sag, southern Songliao Basin, NE China. *Pet. Explor. Dev.* **2021**, *48*, 608–624. [[CrossRef](#)]
17. Gong, L.; Wang, J.; Gao, S.; Fu, X.F.; Liu, B.; Miao, F.B.; Zhou, F.B.; Meng, Q.K. Characterization, controlling factors and evolution of fracture effectiveness in shale oil reservoirs. *J. Pet. Sci. Eng.* **2021**, *203*, 108655. [[CrossRef](#)]
18. Laubach, S.E.; Lander, R.H.; Criscenti, L.J.; Anovitz, L.M.; Urai, J.L.; Pollyea, R.M.; Hooker, J.N.; Narr, W.; Evans, M.A.; Kerisit, S.N.; et al. The Role of Chemistry in Fracture Pattern Development and Opportunities to Advance Interpretations of Geological Materials. *Rev. Geophys.* **2019**, *57*, 1065–1111. [[CrossRef](#)]
19. Gong, L.; Gao, S.; Fu, X.F.; Chen, S.M.; Lyu, B.Y.; Yao, J.Q. Fracture characteristics and their effects on hydrocarbon migration and accumulation in tight volcanic reservoirs: A case study of the Xujiaweizi fault depression, Songliao Basin, China. *Interpretation* **2017**, *5*, 57–70. [[CrossRef](#)]
20. Zhu, X.M.; Zeng, H.L.; Li, S.L.; Dong, Y.L.; Zhu, S.F.; Zhao, D.N.; Huang, W. Sedimentary characteristics and seismic geomorphologic responses of a shallow-water delta in the Qingshankou Formation from the Songliao Basin, China. *Mar. Pet. Geol.* **2017**, *79*, 131–148. [[CrossRef](#)]
21. Liu, B.; Bai, H.L.; Chi, Y.A.; Jia, R.; Fu, X.F.; Yang, L. Geochemical characterization and quantitative evaluation of shale oil reservoir by two-dimensional nuclear magnetic resonance and quantitative grain fluorescence on extract: A case study from the Qingshankou Formation in Southern Songliao Basin, northeast. *Mar. Pet. Geol.* **2019**, *109*, 561–573. [[CrossRef](#)]
22. Huo, Q.; Zeng, H.; Zhang, X.C.; Fang, Q.H.; Wang, Z.Y.; Fu, L. Shale Oil Occurrence and Reservoir Characteristics of the Qijia-Gulong Depression in Songliao Basin. *Acta Geol. Sin.-Engl. Ed.* **2015**, *89*, 151–153. [[CrossRef](#)]
23. Marrett, R.; Gale, J.F.W.; Gómez, L.A.; Laubach, S.E. Correlation analysis of fracture arrangement in space. *J. Struct. Geol.* **2018**, *108*, 16–33. [[CrossRef](#)]
24. Hooker, J.N.; Laubach, S.E.; Marrett, R. Fracture-aperture size–frequency, spatial distribution, and growth processes in strata-bounded and non-strata-bounded fractures, Cambrian Mesón Group, NW Argentina. *J. Struct. Geol.* **2013**, *54*, 54–71. [[CrossRef](#)]
25. Li, J.Z.; Laubach, S.E.; Gale, J.F.W.; Marrett, R. Quantifying opening-mode fracture spatial organization in horizontal wellbore image logs, core and outcrop: Application to Upper Cretaceous Frontier Formation tight gas sandstones, USA. *J. Struct. Geol.* **2018**, *108*, 137–156. [[CrossRef](#)]
26. Gale, J.F.W.; Elliott, S.J.; Rysak, B.G.; Ginn, C.L.; Zhang, N.; Myers, R.D.; Laubach, S.E. Fracture description of the HFTS-2 slant core, Delaware Basin, West Texas. In Proceedings of the Unconventional Resources Technology Conference, Houston, TX, USA, 26 July 2021; Volume 6, pp. 26–28.
27. Finn, M.D.; Gross, M.R.; Eyal, Y.; Draper, G. Kinematics of throughgoing fractures in jointed rocks. *Tectonophysics* **2003**, *376*, 151–166. [[CrossRef](#)]
28. Gong, L.; Gao, M.Z.; Zeng, L.B.; Fu, X.F.; Gao, Z.Y.; Gao, A.; Zhu, K.W.; Yao, J.Q. Controlling factors on fracture development in the tight sandstone reservoirs: A case study of Jurassic-Neogene in the Kuqa foreland basin. *J. Nat. Gas Geosci.* **2017**, *28*, 199–208.
29. Cooke, M.L.; Simo, J.A.; Underwood, C.A.; Rijken, P. Mechanical stratigraphic controls on fracture patterns within carbonates and implications for groundwater flow. *Sediment. Geol.* **2006**, *184*, 225–239. [[CrossRef](#)]
30. Gross, M.R.; Eyal, Y. Throughgoing fractures in layered carbonate rocks. *GSA Bull.* **2007**, *119*, 1387–1404. [[CrossRef](#)]
31. Zhu, H.Y.; Song, Y.J.; Tang, X.H. Research progress on 4-dimensional stress evolution and complex fracture propagation of infill wells in shale gas reservoirs. *Pet. Sci. Bull.* **2021**, *3*, 396–416.
32. Zeng, L.B.; Zhu, R.K.; Gao, Z.Y.; Gong, L.; Liu, G.P. Structural diagenesis and its petroleum geological significance. *Pet. Sci. Bull.* **2016**, *2*, 191–197.
33. Ding, W.L.; Dai, P.; Zhu, D.W.; Zhang, Y.Q.; He, J.H.; Li, A.; Wang, R.Y. Fractures in continental shale reservoirs: A case study of the Upper Triassic strata in the SE Ordos Basin, Central China. *Geol. Mag.* **2016**, *153*, 663–680. [[CrossRef](#)]
34. Wang, W.D.; Zheng, D.; Sheng, G.L.; Zhang, Q.; Su, Y.L. A review of stimulated reservoir volume characterization for multiple fractured horizontal well in unconventional reservoirs. *Adv. Geo-Energy Res.* **2017**, *1*, 54–63. [[CrossRef](#)]
35. Lyu, W.Y.; Zeng, L.B.; Zhang, B.J.; Miao, F.B.; Lyu, P.; Dong, S.Q. Influence of natural fractures on gas accumulation in the Upper Triassic tight gas sandstones in the northwestern Sichuan Basin, China. *Mar. Pet. Geol.* **2017**, *83*, 60–72. [[CrossRef](#)]
36. Gong, L.; Fu, X.F.; Wang, Z.S.; Gao, S.; Jabbari, H.D.; Yue, W.T.; Liu, B. A new approach for characterization and prediction of natural fracture occurrence in tight-oil sandstones with intense anisotropy. *AAPG Bull.* **2019**, *103*, 1383–1400. [[CrossRef](#)]
37. Liu, B.; Song, Y.B.; Zhu, K.; Su, P.; Ye, X.; Zhao, W.C. Mineralogy and element geochemistry of salinized lacustrine organic-rich shale in the middle Permian Santanghu Basin: Implications for paleoenvironment, provenance, tectonic setting and shale oil potential. *Mar. Pet. Geol.* **2020**, *120*, 104569. [[CrossRef](#)]
38. Zeng, L.B.; Tang, X.M.; Wang, T.C.; Gong, L. The influence of fracture cements in tight Paleogene saline lacustrine carbonate reservoirs, Western Qaidam Basin, Northwest China. *AAPG Bull.* **2020**, *96*, 2003–2017. [[CrossRef](#)]
39. Gale, J.F.W.; Fall, A.; Yurchenko, I.A.; Ali, W.A.; Laubach, S.E.; Eichhubl, P.; Bodnar, R.J. Opening-mode fracturing and cementation during hydrocarbon generation in shale: An example from the Barnett Shale, Delaware Basin, West Texas. *AAPG Bull.* **2022**, *106*, 2103–2141.

40. Aydin, A. Failure modes of shales and their implications for natural and man-made fracture assemblages. *AAPG Bull.* **2014**, *98*, 2391–2409. [[CrossRef](#)]
41. Wang, R.Y.; Gu, Y.; Ding, W.L.; Gong, D.J.; Yin, S.; Wang, X.H.; Zhou, X.H.; Li, A.; Xiao, Z.K.; Cui, Z.X. Characteristics and dominant controlling factors of organic-rich marine shales with high thermal maturity: A case study of the Lower Cambrian Niutitang Formation in the Cen'gong block, southern China. *J. Nat. Gas Sci. Eng.* **2016**, *33*, 81–96. [[CrossRef](#)]
42. Laubach, S.E.; Olson, J.E.; Gross, M.R. Mechanical and fracture stratigraphy. *AAPG Bull.* **2009**, *93*, 1413–1426. [[CrossRef](#)]
43. Ferrill, D.A.; McGinnis, R.N.; Morris, A.P.; Smart, K.J.; Sickmann, Z.T.; Bentz, M.; Lehrmann, D.; Evans, M.A. Control of mechanical stratigraphy on bed-restricted jointing and normal faulting. *Eagle Form. South-Cent. Tex. AAPG Bull.* **2014**, *98*, 2477–2506.
44. Zeng, L.B.; Su, H.; Tang, X.M.; Peng, Y.M.; Gong, L. Fractured tight sandstone oil and gas reservoirs: A new play type in the Dongpu depression, Bohai Bay Basin, China. *AAPG Bull.* **2013**, *97*, 363–377. [[CrossRef](#)]
45. Helgeson, D.E.; Aydin, A. Characteristics of joint propagation across layer interfaces in sedimentary rocks. *J. Struct. Geol.* **1991**, *13*, 897–911. [[CrossRef](#)]
46. Lamarche, J.A.; Lavenu, P.C.; Gauthier, B.D.M.; Guglielmi, Y.; Jayet, O. Relationships between fracture patterns, geodynamics and mechanical stratigraphy in Carbonates (South-East Basin, France). *Tectonophysics* **2012**, *581*, 231–245. [[CrossRef](#)]
47. Petrie, E.S.; Evans, J.P.; Bauer, S.J. Failure of cap-rock seals as determined from mechanical stratigraphy, stress history, and tensile-failure analysis of exhumed analogs. *AAPG Bull.* **2014**, *98*, 2365–2389. [[CrossRef](#)]
48. Ferrill, D.A.; Morris, A.P.; McGinnis, R.N.; Smart, K.J.; Wigginton, S.S.; Hill, N.J. Mechanical stratigraphy and normal faulting. *J. Struct. Geol.* **2017**, *94*, 275–302. [[CrossRef](#)]
49. Corradetti, A.; Tavani, S.; Parente, M.; Iannace, A.; Vinci, F.; Pirmez, C.; Torrieri, S.; Giorgioni, M.; Pignalosa, A.; Mazzoli, S. Distribution and arrest of vertical through-going joints in a seismic-scale carbonate platform exposure (Sorrento peninsula, Italy): Insights from integrating field survey and digital outcrop model. *J. Struct. Geol.* **2018**, *108*, 121–136. [[CrossRef](#)]
50. Procter, A.; Sanderson, D.J. Spatial and layer-controlled variability in fracture networks. *J. Struct. Geol.* **2018**, *108*, 52–65. [[CrossRef](#)]
51. Bai, T.; Pollard, D.D. Fracture spacing in layered rocks: A new explanation based on the stress transition. *J. Struct. Geol.* **2000**, *22*, 43–57. [[CrossRef](#)]
52. Wang, R.Y.; Hu, Z.Q.; Liu, J.T.; Wang, X.H.; Gong, D.J.; Yang, T. Comparative analysis of characteristics and controlling factors of fractures in marine and continental shales: A case study of the Lower Cambrian in Cengong area, northern Guizhou Province. *J. Oil Gas Geol.* **2018**, *39*, 631–640.
53. Cao, D.S.; Zeng, L.B.; Lyu, W.Y.; Xu, X.; Tian, H. Progress in brittleness evaluation and prediction methods in unconventional reservoirs. *Pet. Sci. Bull.* **2021**, *01*, 31–45.
54. Agosta, F.; Wilson, C.; Aydin, A. The role of mechanical stratigraphy on normal fault growth across a Cretaceous carbonate multi-layer, central Texas (USA). *Ital. J. Geosci.* **2015**, *134*, 423–441. [[CrossRef](#)]
55. Zeng, L.B.; Wang, H.J.; Gong, L.; Li, B.M. Impacts of the tectonic stress field on natural gas migration and accumulation: A case study of the Kuqa Depression in the Tarim Basin, China. *Mar. Pet. Geol.* **2010**, *27*, 1616–1627. [[CrossRef](#)]
56. Wang, R.Y.; Hu, Z.Q.; Zhou, T.; Bao, H.Y.; Wu, J.; Du, W.; He, J.H.; Wang, W.P.; Chen, Q. Characteristics of fractures and their significance for reservoirs in Wufeng-Longmaxi shale, Sichuan Basin and its periphery. *J. Oil Gas Geol.* **2021**, *42*, 1295–1306.
57. Choi, J.; Edwards, P.; Ko, K.; Kim, Y. Definition and classification of fault damage zones: A review and a new methodological approach. *Earth-Sci. Rev.* **2016**, *152*, 70–87. [[CrossRef](#)]
58. Dimmen, V.; Rotevatn, A.; Peacock, D.C.P.; Nixon, C.W.; Nærland, K. Quantifying structural controls on fluid flow: Insights from carbonate-hosted fault damage zones on the Maltese Islands. *J. Struct. Geol.* **2017**, *101*, 43–57. [[CrossRef](#)]
59. Peacock, D.C.; Dimmen, P.V.; Rotevatn, A.; Sanderson, D.J. A broader classification of damage zones. *J. Struct. Geol.* **2017**, *102*, 179–192. [[CrossRef](#)]
60. Berg, S.S.; Skar, T. Controls on damage zone asymmetry of a normal fault zone: Outcrop analyses of a segment of the Moab fault, SE Utah. *J. Struct. Geol.* **2005**, *27*, 1803–1822. [[CrossRef](#)]
61. Faulkner, D.R.; Jackson, C.A.L.; Lunn, R.J.; Schlische, R.W.; Shipton, Z.K.; Wibberley, C.A.J.; Withjack, M.O. A review of recent developments concerning the structure, mechanics and fluid flow properties of fault zones. *J. Struct. Geol.* **2010**, *32*, 1557–1575. [[CrossRef](#)]
62. Torabi, A.; Berg, S.S. Scaling of fault attributes: A review. *Mar. Pet. Geol.* **2011**, *28*, 1444–1460. [[CrossRef](#)]
63. Bons, P.D.; Elburg, M.A.; Gomez-Rivas, E. A review of the formation of tectonic veins and their microstructures. *J. Struct. Geol.* **2012**, *43*, 33–62. [[CrossRef](#)]
64. Gong, L.; Su, X.C.; Gao, S.; Fu, X.F.; Jabbari, H.; Wang, X.X.; Liu, B.; Yue, W.T.; Wang, Z.S.; Gao, A. Characteristics and formation mechanism of natural fractures in the tight gas sandstones of Jiulongshan Gas Field, China. *J. Pet. Sci. Eng.* **2019**, *175*, 1112–1121. [[CrossRef](#)]
65. Gudmundsson, A.; Kusumoto, S.; Simmenes, T.H.; Philipp, S.L.; Larsen, B.; Lotveit, I.F. Effects of overpressure variations on fracture apertures and fluid transport. *Tectonophysics* **2012**, *581*, 220–230. [[CrossRef](#)]
66. Zeng, L.B.; Gong, L.; Guan, C.; Zhang, B.J.; Wang, Q.Q.; Zeng, Q.; Lyu, W.Y. Natural fractures and their contribution to tight gas conglomerate reservoirs: A case study in the northwestern Sichuan Basin, China. *J. Pet. Sci. Eng.* **2022**, *210*, 110028. [[CrossRef](#)]